Supplemental Figure S1. GTP-dependent and direct interaction between Varp and Rab32. (A) GTP-dependent interaction between Varp and Rab32. Binding assay was performed in the presence of 0.5 mM GTPγS (lane 1) or 1 mM GDP (lane 2) as described in Figure 2A. (B) Direct interaction between Varp and Rab32. Agarose beads coupled with T7-Varp (arrow) were incubated with purified GST-Rab32 (lane 4, closed arrowhead) or GST alone (lane 3, open arrowhead) in the presence of 0.5 mM GTPγS, and bound proteins were detected with Coomassie Brilliant Blue R-250. Input means 1/25 volume of the reaction mixture (lanes 1 and 2). The positions of the molecular mass markers ($\times 10^{-3}$) are shown on the left.

Supplemental Figure S2. Colocalization of Varp and Rab32 in melanocytes. Melan-a cells transiently expressing GFP-Rab32 and Str-Varp (A-D), GFP-Rab32 and Str-Varp-N+VPS9 (E-H), GFP-Rab32 and Str-Varp-ANKR1 (I-L), or GFP-Rab32 and Str-Varp-Δ (M-P). Note that Varp-Full and Varp-ANKR1 colocalized well with Rab32 (yellow in C and K), but that Varp-N+VPS9 or Varp-Δ did not. The insets show magnified views of the boxed area. Only a few Varp- and Rab32-positive signals colocalized with melanosomes (pseudo-colored in blue; arrowheads) in the perinuclear region (but see Supplemental Figure S3; colocalization between Varp and melanosomes were observed in the cell periphery). Scale bars, 20 μm.

Supplemental Figure S3. Colocalization of Varp and Tyrp1 or mature melanosomes in melanocytes. Melan-a cells transiently expressing GFP-Rab32 and Str-Varp were stained

with anti-Tyrp1. Note that Str-Varp (in red) and Tyrp1 (in green) were well colocalized throughout the cytoplasm in melan-a cells (yellow signals in D, arrow and arrowhead), whereas colocalization between Varp and mature melanosomes (pseudo-colored in blue) was only observed in the peripheral region of the cell (E(ii), arrow), but not in the perinuclear region (E(i), arrowhead). The insets show magnified views of the boxed areas (i) and (ii). Scale bar, 20 μm.

Supplemental Figure S4. Effect of the *Varp* shRNA site 2 on Tyrp1 staining and distribution in melan-a cells. Melan-a cells were transfected with *Varp* shRNA site 2 expression vector together with the GFP expression vector as a transfection marker. Cells were immunostained with anti-Tyrp1 antibody and visualized with Alexa Fluor 594 secondary antibody. Bright-field images show the melanosome distribution in the cells. Scale bar, 20 μm. Note that shRNA (site 2)-mediated knockdown of Varp also dramatically reduced Tyrp1-staining (arrowheads) in melan-a cells.

Supplemental Figure S5. Effect of Varp-ANKR1-Δ on expression and distribution of Tyrp1 in melanocytes. (A) Expression of Varp-ANKR1-Δ in melan-a cells had no effect on Tyrp1 staining or its distribution. Scale bar, 20 μm. (B) Quantitative immunofluorescence analysis indicated that expression of the Rab32/38-binding-defective mutant ANKR1-Δ had no effect on expression of Tyrp1 in melan-a cells. The bars represent the means ± S.E. of data from three independent dishes ($n > 50$).

Supplemental Figure S6. Effect of constitutive active/negative Rab21 mutants (A, a-h) and *Rab21* shRNA (A, i-l) on expression and distribution of Tyrp1 in melanocytes. Melan-a cells were transfected with pEGFP-C1-Rab21-Q76L/T31N or with *Rab21* shRNA (target sequence: 5'-TTTACTACCGAGATTCGAA-3') expression vector together with the GFP expression vector as a transfection marker. Cells were immunostained with anti-Tyrp1 antibody and visualized with Alexa Fluor 594 secondary antibody. Bright-field images show the melanosome distribution in the cells. Scale bars, 20 μm. (B) Efficiency and specificity of shRNA targeted against Rab21 were confirmed in COS-7 cells as described in Figure 6A.

Supplemental Figure S7. Proteasome-dependent degradation of Tyrp1 in Varp-deficient melanocytes. (A) Melan-a cells were transfected with *Varp* shRNA expression vector together with the GFP expression vector as a transfection marker, treated with either DMSO (control; a-d), a proteasome inhibitor (MG132; e-h), or lysosomal protease inhibitors (E64d and pepstatin A; i-l), and stained with anti-Tyrp1 antibody. Note that treatment of the cells with MG132, but not with the lysosomal protease inhibitors, restored Tyrp1 signals. Scale bars, 20 μm. (B) MG132-dependent recovery of Tyrp1 signals in *Varp*-siRNA-expressing melanocytes as revealed by immunofluorescence analysis. Note that expression of Tyrp1 in *Varp*-siRNA-expressing cells was restored to a level comparable to the level in the control untransfected cells. The bars represent the means ± S.E. of data from three independent dishes ($n > 50$). **, $p < 0.01$ (Student's unpaired t test). (C) MG132-dependent recovery of Tyrp1

expression in *Varp*-siRNA-expressing melanocytes as revealed by immunoblotting. Cell lysates of melan-a cells expressing either *Varp* siRNA or control siRNA (approximately 30 μg) were subjected to 10% SDS-PAGE followed by immunoblotting with anti-Tyrp1 antibody (1/200 dilution) and anti-actin antibody (1/400 dilution). The positions of the molecular mass markers ($\times 10^{-3}$) are shown on the left.

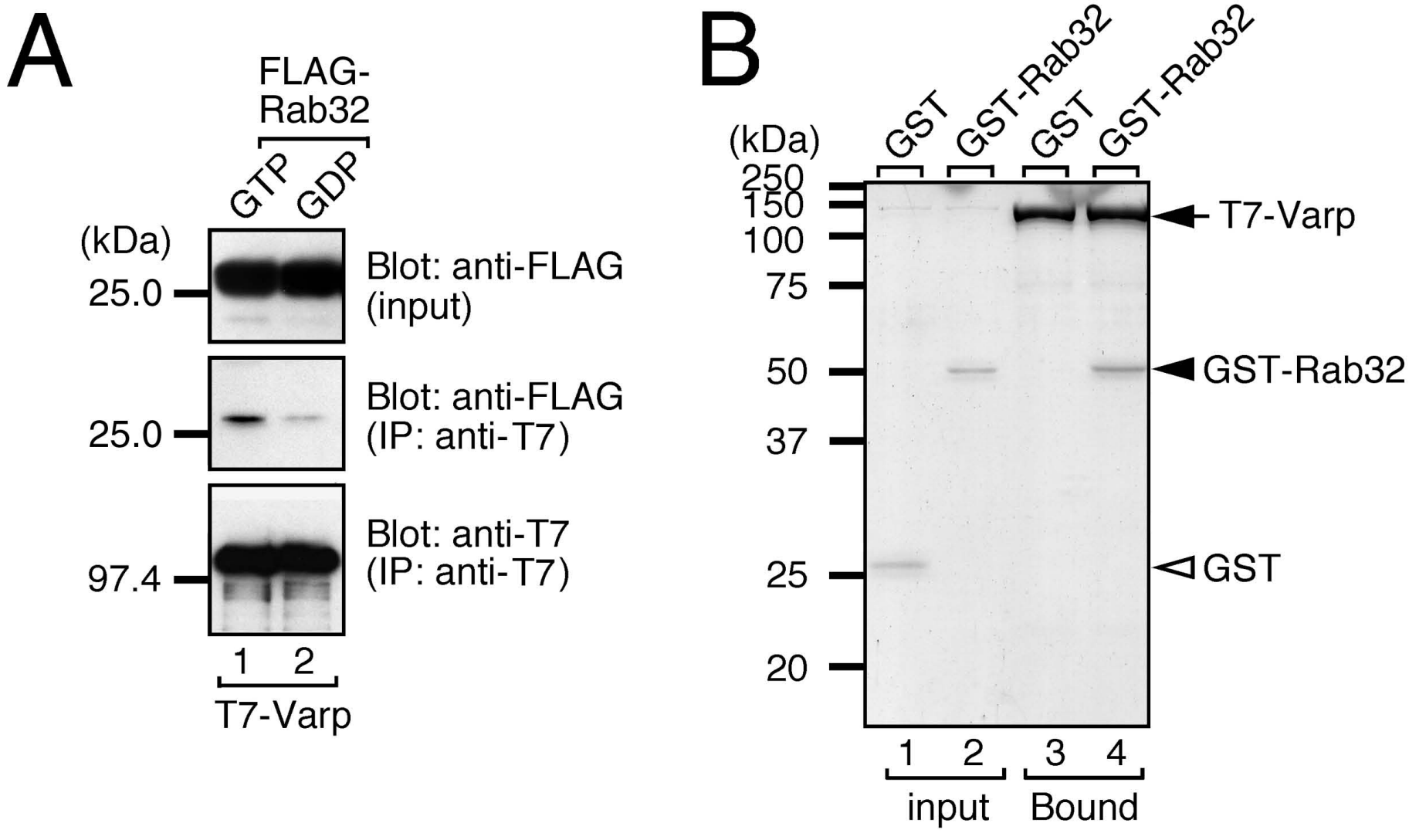

Tamura *et al.*, Supplemental Fig. S1, Top ⇑

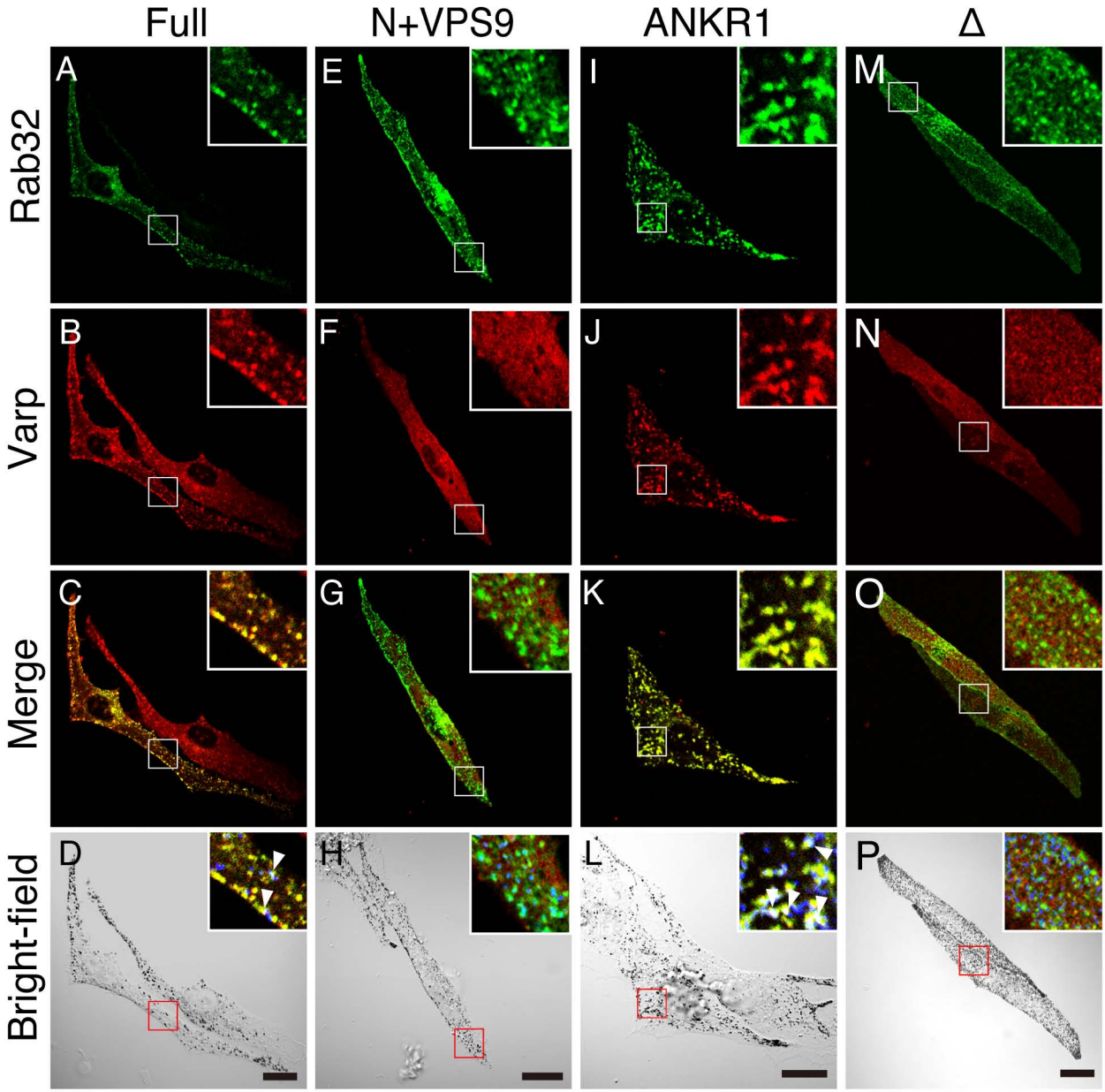

Tamura *et al.*, Supplemental Fig. S2, Top ⇑

Tamura *et al.*, Supplemental Fig. S3, Top ⇑

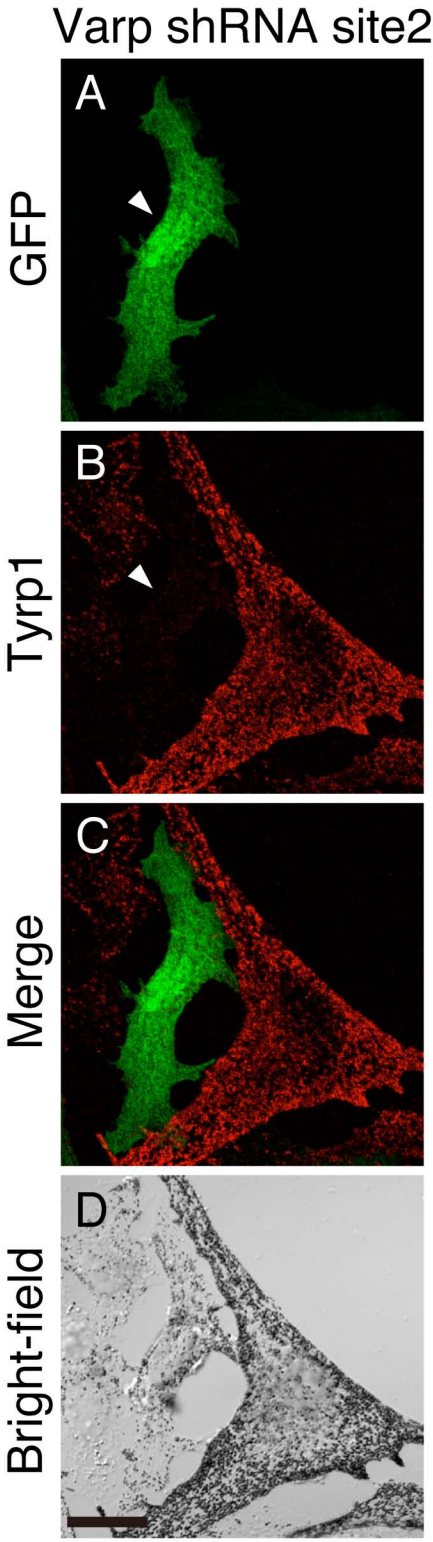

Tamura *et al.*, Supplemental Fig. S4, Top ⇑

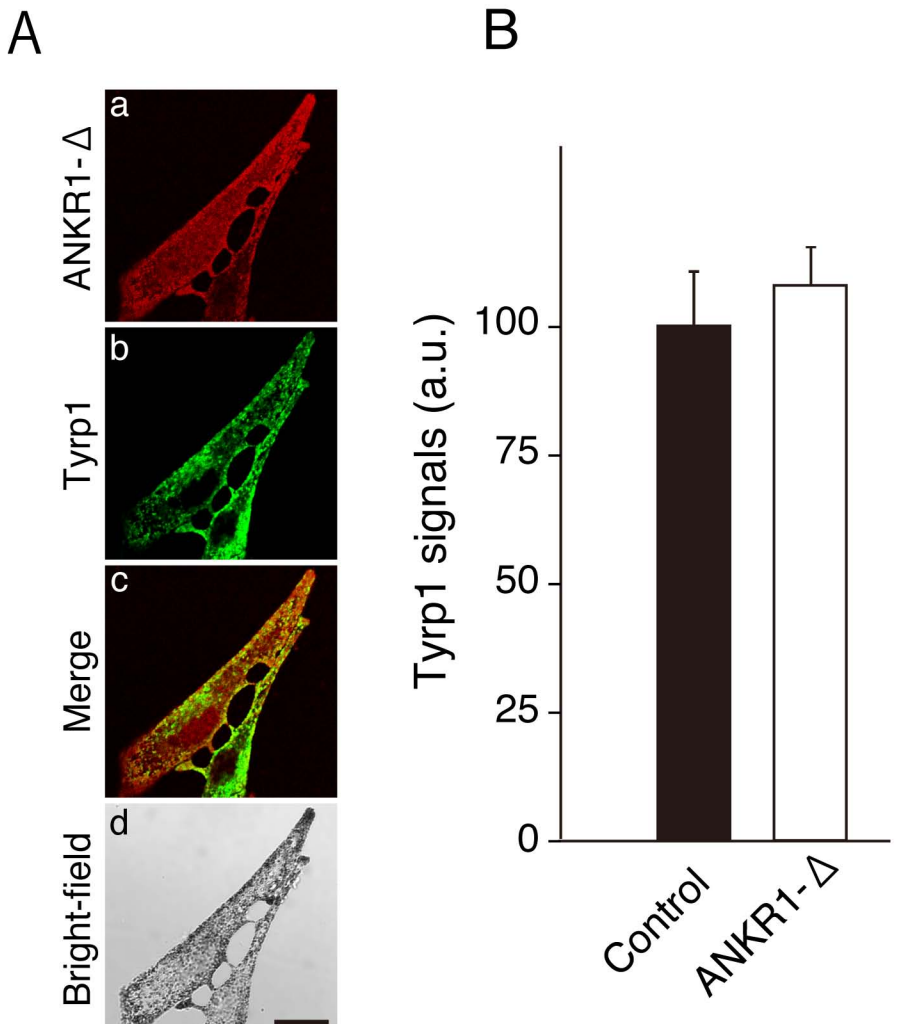

Tamura *et al.*, Supplemental Fig. S5, Top ⇑

A

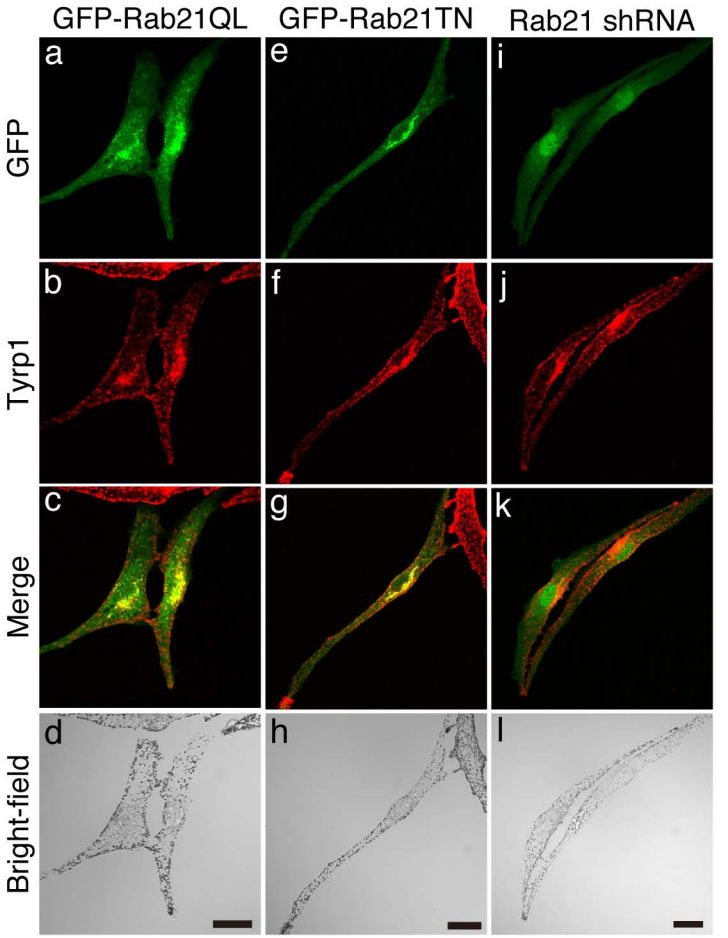

B

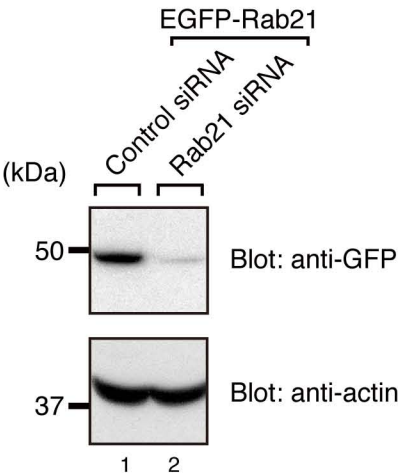

Tamura *et al.*, Supplemental Fig. S6, Top ⇑

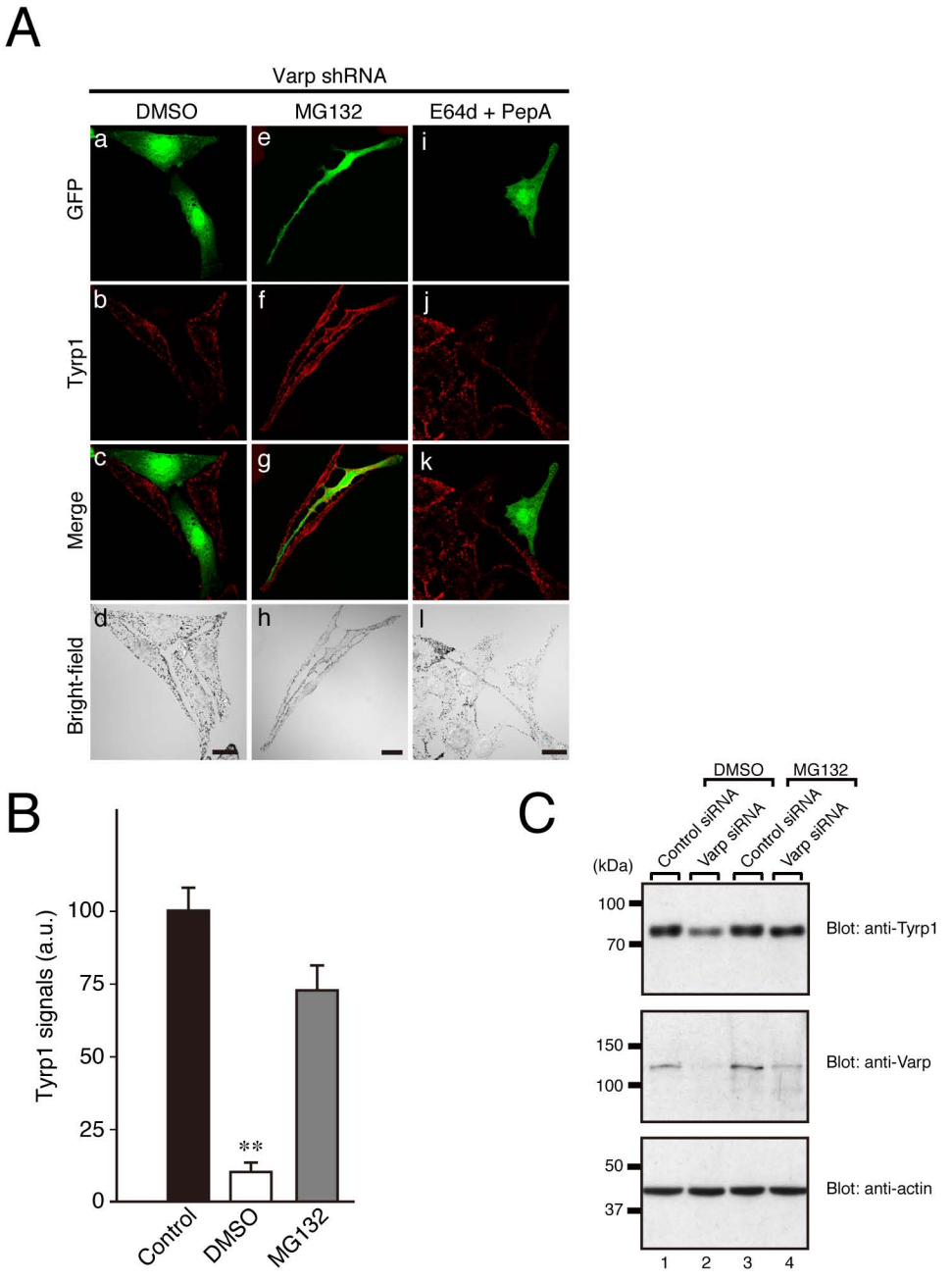

Tamura *et al.*, Supplemental Fig. S7, Top ⇑